ORIGINAL PAPER

Relation Between Particle Properties and Rheological Characteristics of Carrot-derived Suspensions

**Katlijn R. N. Moelants · Ruth Cardinaels · Ruben P. Jolie · Tina A. J. Verrijssen ·
Sandy Van Buggenhout · Lourdes M. Zumalacarregui · Ann M. Van Loey ·
Paula Moldenaers · Marc E. Hendrickx**

Abstract The effect of particle properties on the rheological behaviour of carrot-derived suspensions was investigated systematically. Hereto, a range of relatively monodisperse suspensions, with varying average particle sizes (~73, 176, 262 and 369 μm) and pulp contents (from 30 to 65 wt.%), was prepared by the reconstitution of carrot tissue particles in water. Suspensions with average particle size of ~73 μm consisted of cell fragments, whereas suspensions with larger particle sizes contained mainly cell clusters of which the cell number increased with increasing particle size. The rheological characteristics showed that the carrot-derived suspensions have a non-Newtonian behaviour with a yield stress, depending on particle concentration, size and type. The network structure of all suspensions could be described as a weak gel. Increase in yield stress and storage modulus with particle concentration could be fitted to a power law model. A unique linear relation was found between the yield stress and the plateau modulus, independent of the particle size and type. Particle concentration, size and type appeared to be key structural parameters controlling the rheology of these carrot-derived suspensions. When comparing the rheological behaviour of the reconstituted suspensions with the original carrot purée of similar average diameter and pulp content, the network structure (measured as yield stress or storage modulus) in carrot purée was weaker, which may be attributed to the broader particle size distribution.

Keywords Rheology · Microstructure · Carrot purée · Reconstitution · Particle properties

Introduction

Nowadays, large amounts of raw vegetables are processed into derived liquid products such as soups, juices and purées. The quality of these products (e.g. with regard to texture, bioaccessibility of micronutrients and flavour release), important for producers and consumers, is determined by their microstructure and the related rheology (Bayod et al. 2005). Hence, understanding the relation between the microstructure and the rheological properties of these products is needed to allow tailoring their quality characteristics.

Vegetable juices, purées and soups are plant-based food suspensions consisting of plant tissue-based particles in a continuous serum phase with (among others) pectin, sugars and organic acids solubilised in it (Rao 1987; Anthon et al. 2008). Their rheological properties are known to be determined by both the particle properties of the dispersed

K. R. N. Moelants · R. P. Jolie · T. A. J. Verrijssen ·
S. Van Buggenhout · A. M. Van Loey · M. E. Hendrickx (✉)
Laboratory of Food Technology and Leuven Food Science
and Nutrition Research Centre (LFoRCe), Department
of Microbial and Molecular Systems (M2S), Katholieke
Universiteit Leuven,
Kasteelpark Arenberg 22, PB 2457, 3001 Leuven, Belgium
e-mail: Marc.Hendrickx@biw.kuleuven.be

R. Cardinaels · P. Moldenaers
Laboratory of Applied Rheology and Polymer Processing,
Department of Chemical Engineering,
Katholieke Universiteit Leuven,
Willem de Croylaan 46, PB 2423, 3001 Leuven, Belgium

L. M. Zumalacarregui
Process Analysis Research Group, Chemical Engineering Faculty,
Higher Polytechnic Institute Jose Antonio Echeverria,
114 St. 11901 Marianao,
CP 19390 Havana, Cuba

phase and the properties of the serum phase (especially of the solubilised pectin) (Tanglertpaibul and Rao 1987a; Yoo and Rao 1994; Beresovsky et al. 1995; Den Ouden and Van Vliet 1997; Servais et al. 2002; Valencia et al. 2003; Anthon et al. 2008). The particle properties that affect the rheology of the suspension include the concentration, size distribution, shape, surface properties, deformability and interparticle forces (Gallegos et al. 2004; Genovese et al. 2007; Fischer et al. 2009). In non-food suspension rheology, most authors focussed on the effect of particle properties for suspensions with spherical and/or rigid particles (Larson 1995; Mewis and Wagner 2011). However, because of the irregular, deformable character of particles from cellular material, the rheology of food suspensions is much more complex than that of suspensions of monodisperse, solid spheres. Moreover, interactions between the suspended particles and the continuous serum phase can occur, which further complicates the study of the rheology of food suspensions (Errington et al. 1998).

To study the rheology of suspensions, both steady-shear and oscillatory tests can be performed. The first type of test serves to obtain insight into the flow and processing behaviour of suspensions, whereas in the second type of test, the viscoelastic behaviour of suspensions is investigated (Steffe 1996). With regard to flow, a non-Newtonian behaviour is very common in fruit- and vegetable-derived products (Rao 2007). For example, shear thinning or thickening can occur and can be studied by fitting the flow curves of the suspensions to predictive models (e.g. the Herschel–Bulkley model). Estimated values of the model parameters can then be used to characterise the flow behaviour of the suspensions. Besides this shear rate dependence of the viscosity, fruit- and vegetable-based products often possess a critical stress below which no flow can be observed, referred to as the yield stress. Since the yield stress provides a measure for the structure of the material (Steffe 1996; Tabilo-Munizaga and Barbosa-Canovas 2005), this rheological parameter is also important for the characterisation of the flow behaviour of suspensions. According to Cheng (1986), the yield stress measured in an undisrupted sample is the static yield stress, while the yield stress of a sample with completely broken-down structure, often determined from extrapolation of flow curves to zero shear rate, is the dynamic yield stress. In most studies on food suspensions, only one of these two is studied and differences between them are unfortunately ignored. To characterise the viscoelastic behaviour of suspensions, storage and loss moduli are typically obtained from oscillatory tests. The storage modulus at low frequencies can be used as a measure for network stiffness, while the ratio of the loss modulus to the storage modulus gives insight into the network type (Steffe 1996; Day et al. 2010b).

Despite its importance for tailoring food quality, unambiguous knowledge about the relations between particle properties and rheology of vegetable suspensions is missing at present. In this study, the effect of particle properties on the rheology of carrot-derived suspensions is investigated systematically. In order to extract unambiguous relations between rheological and structural properties, it is important to use well-characterised samples. Hereto, the reconstitution principle was used to prepare suspensions with various particle concentrations and well-characterised particle size, distinguishing this study from most rheological studies on vegetable suspensions available in literature. High-pressure homogenisation (at different pressure levels) in combination with wet sieving was used as tool to prepare particles with different sizes. Although particle concentration and size were the only two deliberately chosen variables in the reconstitution process, changes in particle size turned out to be accompanied with changes in particle type (in this work referring to cell fragment, cell or cell cluster). Therefore, in the interpretation of the results, particle type will be another variable to take into account. The influence of the serum properties on the rheological characteristics of the food suspension was excluded by reconstituting in water rather than serum. Carrot, a common ingredient in ready-to-eat foods, was selected as a model system. Since particle charge and hence particle interactions are affected by pH, the carrot-derived suspensions, having almost neutral pH, can serve as model systems for other plant-based suspensions with neutral pH.

The aim of this study was to identify the rheological parameters that can characterise the structure of the plant-based suspensions and vice versa. Attempts will be made to define several quantitative relations between structural properties and rheological parameters of the reconstituted carrot-derived suspensions. These relations can be helpful in understanding and predicting the flow behaviour of carrot purées with different structural properties.

Materials and Methods

Plant Material

Fresh carrots (*Daucus carota* cv. Nerac) were purchased from a local supplier in Belgium and stored at 4 °C until further use.

Preparation of Carrot-derived Suspensions

For the preparation of the reconstituted suspensions, carrots were peeled and cut into pieces. The pieces were heated in a temperature-controlled water bath at 95 °C

for 5 min (to inactivate intrinsic enzymes). After heating, the carrot pieces were immediately cooled in an ice water bath. Subsequently, they were mixed with deionised water in a 1:1 ratio to facilitate the blending process, which was performed during 1 min using a blender (Waring blender 7010G, Torrington, CT, USA). The carrot blend was further disintegrated with a high-pressure homogeniser (Panda 2K, Gea Niro Soavi, Mechelen, Belgium) at two different pressures (20 or 100 MPa). A single batch of heated and blended carrots was used to prepare all carrot purées homogenised at the same pressure.

Purées obtained after homogenisation were further processed to prepare reconstituted carrot-derived suspensions with different particle sizes and particle concentrations. After homogenisation, purées were separated in fractions with different particle sizes by using the technique of wet sieving (Retsch, Aartselaar, Belgium) with a set of sieves with pore sizes of 40, 80, 125, 250, 500 and 1,000 μm. For the purée homogenised at 20 MPa, the pulp retained on the sieves with pore sizes of 125 and 250 μm was collected, whereas for the purée homogenised at 100 MPa, the pulp retained on the sieves with pore sizes of 40 and 125 μm was assembled. Pulp was drained over a filter to remove excess water until constant weight was reached. These pulp fractions were stored at 4 °C (for maximally 2 weeks).

At the moment of further analysis, the pulp was reconstituted with deionised water in different pulp percentages (pulp%; ranging from 30 to 65 wt.%), resulting in

reconstituted carrot-derived suspensions. The pulp% was defined as:

$$pulp\%(\%) = \frac{\text{mass of pulp}}{\text{mass of pulp and water}} \times 100 \qquad (1)$$

Figure 1 gives a schematic overview of the reconstitution process.

For the preparation of the original carrot purées, carrots were also peeled and cut into pieces. However, before the heat treatment, pieces were vacuum-packed in plastic bags to avoid loss of solubilised pectin in the heating water. Packed samples were heated at 95 °C for 5 min, cooled, blended and homogenised at 20 or 100 MPa. These original carrot purées were stored at 4 °C until further analysis (maximally 1 week).
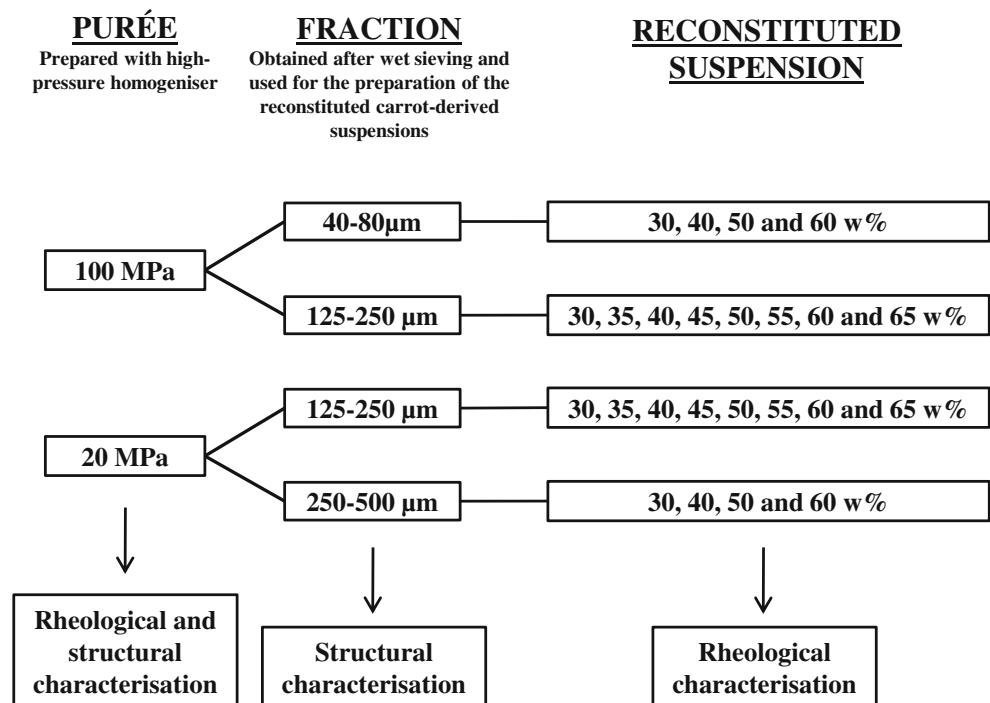
Sample coding for the reconstituted suspensions and the original carrot purée is summarised in Table 1.

Structural Characterisation of the Particles

Particle size Distribution

The particle size distribution (PSD) of the suspensions was measured using laser diffraction (Malvern Instrument Ltd., Worcestershire, UK), which can detect particles between 0.05 and 880 μm. Approximately 6 g of sample (50 wt.%) was poured in a stirred tank filled with deionised water. The diluted sample was pumped into the measuring cell. The volumetric PSDs were calculated from the intensity profile

Fig. 1 Schematic overview of the preparation and reconstitution of carrot-derived suspensions from carrot purée

PURÉE Prepared with high-pressure homogeniser	**FRACTION** Obtained after wet sieving and used for the preparation of the reconstituted carrot-derived suspensions	**RECONSTITUTED SUSPENSION**

100 MPa
- 40-80μm → 30, 40, 50 and 60 w%
- 125-250 μm → 30, 35, 40, 45, 50, 55, 60 and 65 w%

20 MPa
- 125-250 μm → 30, 35, 40, 45, 50, 55, 60 and 65 w%
- 250-500 μm → 30, 40, 50 and 60 w%

Rheological and structural characterisation

Structural characterisation

Rheological characterisation

Table 1 Sample coding and preparation conditions

Sample code	Preparation conditions
Carrot purée	
P_20	Carrot H+B+HPH 20 MPa
P_100	Carrot H+B+HPH 10 MPa
Reconstituted suspensions	
RS_40μm(100)_30%	Carrot H+B+HPH 100 MPa+W 40 μm+R 30 wt.%
RS_40μm(100)_40%	Carrot H+B+HPH 100 MPa+W 40 μm+R 40 wt.%
RS_40μm(100)_50%	Carrot H+B+HPH 100 MPa+W 40 μm+R 50 wt.%
RS_40μm(100)_60%	Carrot H+B+HPH 100 MPa+W 40 μm+R 60 wt.%
RS_125μm(20)_30%	Carrot H+B+HPH 20 MPa+W 125 μm+R 30 wt.%
RS_125μm(20)_35%	Carrot H+B+HPH 20 MPa+W 125 μm+R 35 wt.%
…	…
RS_125μm(20)_65%	Carrot H+B+HPH 20 MPa+W 125 μm+R 65 wt.%
RS_125μm(100)_30%	Carrot H+B+HPH 100 MPa+W 125 μm+R 30 wt.%
RS_125μm(100)_35%	Carrot H+B+HPH 100 MPa+W 125 μm+R 35 wt.%
…	…
RS_125μm(100)_65%	Carrot H+B+HPH 100 MPa+W 125 μm+R 65 wt.%
RS_250μm(20)_30%	Carrot H+B+HPH 20 MPa+W 250 μm+R 30 wt.%
RS_250μm(20)_40%	Carrot H+B+HPH 20 MPa+W 250 μm+R 40 wt.%
RS_250μm(20)_50%	Carrot H+B+HPH 20 MPa+W 250 μm+R 50 wt.%
RS_250μm(20)_60%	Carrot H+B+HPH 20 MPa+W 250 μm+R 60 wt.%

H heated at 95 °C for 5 min, *B* blending for 1 min, *HPH* high-pressure homogenisation at 20 or 100 MPa, *W* wet sieving with pore size of sieve from which pulp is collected, *R* reconstitution with mass ratio of pulp to water in weight percent

of the scattered light with the Mie theory by use of the instrument's software. Parameters $D[v,0.1]$, $D[v,0.5]$ and $D[v,0.9]$ (in micrometres) indicate the particle diameter at which 10, 50 and 90 vol.% of the particles have a smaller diameter, respectively. For each sample, also the volume-based ($D[4,3]$) and the area-based ($D[3,2]$) diameter (in micrometres) were determined according to the equations:

$$D[4,3] = \frac{\sum_i n_i d_i^4}{\sum_i n_i d_i^3} \tag{2}$$

$$D[3,2] = \frac{\sum_i n_i d_i^3}{\sum_i n_i d_i^2} \tag{3}$$

where n_i is the number of particles of diameter d_i (in micrometres). All analyses were carried out in duplicate.

The relative width of the PSD, referred to as the spread, was calculated as:

$$\text{spread} = \frac{(D[v,0.9] - D[v,0.1])}{D[3,2]} \tag{4}$$

Total Solid Content

The total solid content of each suspension was determined (using the AOAC official method 20.5 or 30.2) (Horwitz 1980) by drying 3.0±0.1 g of each sample in a vacuum

oven (TCPS, Rotselaar, Belgium) at 70 °C and a pressure of 60 kPa until a constant weight was obtained (±4–5 h). All analyses were conducted in duplicate.

Phase Volume

Samples (20 g) were centrifuged (Beckman J2-HS, Analis, Namen, Belgium) at 12,900×g for 30 min at 20 °C. The phase volume (φ) of the particles in each suspension was determined as:

$$\phi(\%) = \frac{M_p}{M_t} \times 100\% \tag{5}$$

with M_p as the mass of the precipitate (in grammes) and M_t as the total mass of the carrot-derived suspension before centrifugation (in grammes), assuming that the density of the carrot-derived particles was almost equal to that of water. All determinations were carried out in duplicate.

Bright Field Microscopy

Light micrographs were taken using an Olympus BX-41 light microscope equipped with an Olympus XC-50 digital camera (Olympus, Optical Co. Ltd., Tokyo, Japan) and were used to analyse the microstructure of the suspensions. The fractions were diluted tenfold with a toluidine blue solution to stain the cell walls. After 20 min, two droplets of the stained sample were placed on a glass slide (not

covered). The samples were studied using an objective of ×10 or ×40 magnification.

Fluorescence Microscopy

Micrographs were taken using an Olympus BX-41 microscope (Olympus, Optical Co. Ltd., Tokyo, Japan) equipped with epifluorescence illumination (X-CiteR Fluorescence Illumination, Series 120Q, EXFO Europe, Hants, UK). For fluorescence microscopy, the fractions were diluted tenfold and stained with the fluorescent dye acridine orange. Two droplets of the stained sample were placed on a glass slide and studied using an objective of ×10 or ×40 magnification.

Rheological Characterisation of the Suspensions

Prior to the rheological measurements, the stability of the reconstituted suspensions against creaming or sedimentation within a time span of 20 min was checked by use of a Turbiscan MA 2000 (Formulaction SA, l'Union, France). No significant sedimentation was noticed, indicating that sedimentation will be negligible during rheological measurements.

The rheological properties of the suspensions were measured with a stress-controlled rheometer (MCR 501, Anton Paar, Graz, Austria) at 25 °C. As for geometry, a six-bladed vane with a diameter of 11 mm and a height of 16 mm was used to avoid wall slip. Approximately 50 mL of sample was loaded into a cup with 28.92 mm diameter. As it is known that a shear rate distribution occurs by the use of vane geometry, all the shear rates indicated are representative shear rates. Because of the relatively short duration of each measurement (i.e. 20–30 min), evaporation was considered negligible. To avoid the effect of loading history on the structure, samples were pre-sheared for 1 min at a shear rate ($\dot{\gamma}$) of 100 s^{-1} followed by 2 min of rest ($\dot{\gamma} = 0 \, \mathrm{s}^{-1}$) before all measurements.

The rheological characteristics of the suspensions were studied by the execution of steady-shear tests (for the estimation of viscosity and yield stress) and oscillatory tests (to study the viscoelastic behaviour). The former measurements give information about the sample under large deformations. The flow curves (shear stress versus shear rate: $\sigma = f(\dot{\gamma})$) and the viscosity curves (viscosity versus shear rate: $\eta = f(\dot{\gamma})$) were measured by decreasing $\dot{\gamma}$ linearly from 100 to 0.1 s^{-1}. Each shear rate was applied to the sample for 20 s and it was verified that steady-state viscosities were obtained in this way. Thixotropy was checked by the successive execution of a rate sweep up and back down. The hysteresis area between viscosity curves obtained with increasing versus decreasing $\dot{\gamma}$ appeared negligibly small. Hence, irreversible changes in flow behaviour due to particle depletion around the vane blades

at high shear rates, as reported recently by Ovarlez et al. (2011), do not occur for the carrot-derived suspensions under investigation. The static yield stress (σ_{0S}) was determined by the conduction of a stress ramp test from 0.1 Pa until the yield stress was reached. In total, 40 measuring points per decade of the shear stress were obtained and each shear stress was applied for 10 s. The obtained values of σ_{0S} were nearly independent of the number of measuring points and measuring time.

Besides steady-shear tests, oscillatory-shear measurements, during which the oscillatory deformation is small, were performed to obtain information about the sample's network structure at rest. For each sample, an oscillatory strain sweep test was carried out at a constant angular frequency (ω) of 10 rad/s to establish the range of linear viscoelastic response. A frequency sweep test was performed at a constant strain (γ) of 0.1% (within the linear viscoelastic region) from 100 to 0.1 rad/s to determine the frequency dependence of the storage modulus (G') and the loss modulus (G'') of the suspensions.

All measurements were performed in duplicate. For each measurement, a fresh sample was loaded into the cup.

Statistical Analysis

Particle size analyses and rheological measurements were all carried out in duplicate. Results are given as the mean of the two measurements±standard deviation.

The flow curves of the suspensions were fitted to the Bingham and Herschel–Bulkley models (Eqs. 6 and 7, respectively) by the use of linear and non-linear regression procedures, respectively (statistical software package SigmaPlot, version 11, London, UK):

$$\sigma = \sigma_{0D} + \mu \, \dot{\gamma} \tag{6}$$

$$\sigma = \sigma_{0D} + K \dot{\gamma}^n \tag{7}$$

with σ is the shear stress (in pascals), $\dot{\gamma}$ is the shear rate (per second), σ_{0D} is the dynamic yield stress (in pascals), μ is the plastic viscosity (in pascals per second), K is the consistency coefficient (in pascals per second raised to the nth power) and n is the flow index. The data points were fitted without weighing.

To evaluate the effect of particle concentration on rheological parameters such as dynamic and static yield stress and storage modulus, experimental data were fitted to a power law model with two parameters by means of non-linear regression analysis (cf. Eqs. 8, 9 and 13). Also the frequency dependence of G' and G'' was investigated by the use of this type of power law model (cf. Eqs. 11 and 12; SigmaPlot).

Results and Discussion

Preparation of the Suspensions

The relations between the structural (particle) properties and the rheological properties of carrot-derived suspensions have been investigated. Hereto, particles with different particle sizes were reconstituted with water in different concentrations to create reconstituted suspensions with different structural characteristics. The preparation of these reconstituted suspensions proceeded in different steps. To start, original carrot purées were prepared from carrots who first received a thermal treatment (to inactivate enzymes) and were then blended and homogenised in a high-pressure homogeniser (at pressures of 20 or 100 MPa) to disintegrate carrot tissue into carrot particles. In this first step, two kinds of original carrot purées were prepared: one homogenised at 20 MPa (P_20) and the other homogenised at 100 MPa (P_100). In a second step, particles with different sizes were obtained from the original carrot purées by the use of wet sieving (RS_40μm(100), RS_125μm(100), RS_125μm (20), and RS_250μm(20)). Lastly, particles were combined with water in different amounts to prepare the reconstituted carrot-derived suspensions. By using water rather than the serum, possible interference of the pH and the presence of ions and dissolved polymers on the rheology were eliminated. In Fig. 1, the reconstitution process is schematically described.

In what follows, the reconstituted suspensions and the original carrot purées will first be structurally characterised. Subsequently, the rheological characteristics of these suspensions (flow behaviour and viscoelastic behaviour) will be discussed and the relations between the rheological characteristics and the structural properties will be investigated.

Structural Characterisation of the Particles

Particle Size

PSDs were measured by laser diffraction both for the four separated particle fractions and for the original carrot purées homogenised at 20 or 100 MPa. Measurements showed a monomodal size distribution, both for the separated fractions and the purées. The cumulative volumetric PSD of all fractions and both original carrot purées is shown in Fig. 2.

Based on the PSDs, various characteristic diameters could be calculated (Table 2). It is important to mention that values from laser diffraction are calculated assuming spherical particles. These values should be treated with caution because particles in plant suspensions are not spherical. The average particle size, expressed as $D[v,0.5]$,
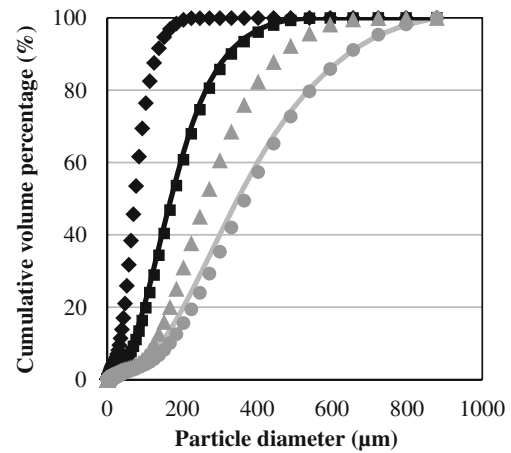
Fig. 2 Cumulative volumetric PSD of RS_40μm(100) (*black diamonds*), RS_125μm(100) (*black squares*), P_100 (*black lines*), RS_125μm(20) (*grey triangles*), RS_250μm(20) (*grey circles*) and P_20 (*grey lines*)

of material retained on the sieves with pore sizes of 40 and 125 μm from purée homogenised at 100 MPa were 73 and 176 μm, respectively. Pulp collected from the sieves with pore sizes of 125 and 250 μm from purée homogenised at 20 MPa possessed average particle sizes of 262 and 369 μm, respectively. $D[v,0.5]$ of P_100 and P_20 were 170 and 350 μm, respectively, which is almost identical to $D[v,0.5]$ of RS_125μm(100) and RS_250μm(20), respectively. The collected pulp thus consists of relatively large particles whereby particle fraction is dominated by non-Brownian particles.

Particle size was also measured as the area-based ($D[3,2]$) or the volume-based diameter ($D[4,3]$). $D[4,3]$ is highly influenced by the presence of large particles, whereas the contribution of small particles to $D[3,2]$ is larger compared to $D[4,3]$. Although values of $D[4,3]$ were larger than those of $D[3,2]$, trends in both parameters were the same. As expected, it can be seen from Table 2 and Fig. 2 that particles of RS_250μm(20) were the largest, whereas those of RS_40μm(100) turned out to be the smallest. Particle size was also larger for particles in RS_125μm(20) in comparison to particles in the same fraction obtained from purées homogenised at 100 MPa. This difference in particle size can be caused by a difference in PSD between the original carrot purées.

The size at which 90 vol.% of the particles have a smaller diameter (i.e. $D[v,0.9]$) (Table 2) for each fraction was larger (~1.3–1.8 times) than expected from the sieve pores (80, 250 or 500 μm). This observation may be explained by the fact that parenchyma cells, accounting for the majority of cells in vegetable suspensions, are highly deformable (Den Ouden and Van Vliet 2002) and by the fact that carrot-derived particles are non-spherical (cf. the "Particle type" section). Hence, they can pass through pores

Table 2 Particle size of the reconstituted carrot-derived suspensions and the original purées expressed as the size of which 10, 50 or 90 vol.% of the particles have a smaller diameter ($D[v,0.1]$, $D[v,0.5]$ and $D[v,0.9]$), the area-based diameter ($D[3,2]$) and the volume-based diameter ($D[4,3]$)

Sample	$D[v,0.5]$ (µm)	$D[v,0.9]$ (µm)	$D[v,0.1]$ (µm)	$D[3,2]$ (µm)	$D[4,3]$ (µm)	Spread
RS_40µm(100)	73	131	33	44	78	2.2
RS_125µm(100)	176	334	75	92	192	2.8
RS_125µm(20)	262	458	127	140	278	2.4
RS_250µm(20)	369	641	167	168	386	2.8
P_20	350	641	106	106	372	5.1
P_100	170	321	67	67	183	3.8

The spread of the PSD is calculated as in Eq. 4

with a smaller size than the size of the particle itself. In addition, only the second smallest dimension should be smaller than the pore size to pass through the sieve. All other dimensions can be larger, as a result of which particles can have a $D[v,0.9]$ larger than the pore size of the sieves they pass.

In addition to these characteristic diameters, also the relative width of the PSD, expressed as the spread, was calculated using Eq. 4. $D[3,2]$ was used for the normalisation in this calculation because $D[4,3]$ and $D[v,0.5]$ are highly influenced by larger particles that can distort the spread. As expected, the spread of the reconstituted suspensions turned out to be smaller than the spread of the original carrot purées.

Particle Type

Carrot tissue cells have an average diameter of 60–70 µm (Zdunek et al. 2007; Day et al. 2010a; Lopez-Sanchez et al. 2011b). Consequently, RS_40µm(100) can be assumed to consist of single cells and cell fragments, while in RS_125µm(100) and RS_125µm(20), small clusters of cells can appear. Large cell clusters can be found in RS_250µm(20). These differences in particle type among the particle fractions were confirmed with micrographs (Fig. 3a–d). On these images and, in more detail, on the micrographs of Fig. 3e–f, particles with rough edges and broken cells rather than separate intact cells are visible. This shows that cell breakage occurred during mechanical breakup rather than cell separation along the middle lamella. Thus, heat treatment of the carrot pieces (95 °C for 5 min) during the production of the carrot purée turned out to be insufficient to degrade pectin in the middle lamella enough to cause cell separation. In what follows, the changes in particle type, accompanying the changes in particle size, are another important factor to take into account when interpreting the rheological results. Other studies reported that different types of particles, such as tissue particles mainly consisting of cell fragments, single cells or clusters of cells, could lead to different functional

properties of materials (Day et al. 2010a, b; Lopez-Sanchez et al. 2011b).

Unfortunately, the micrographs could not be used to describe the structure of the suspensions because the suspensions had to be diluted for microscopic analysis, causing changes in structure.

Particle Concentration

Particle concentration was expressed as the phase volume (φ), the total solid content and the pulp%. However, due to the compressible nature of plant-based suspensions, the value of φ determined by centrifugation may differ from the exact phase volume occupied by the particles in the suspension. Since φ and total solid content were found to be almost proportional to the pulp% (data not shown), the pulp% was chosen here as the parameter to express the particle concentration.

Characterisation of the Flow Behaviour

Qualitative Description of the Non-Newtonian Flow Behaviour

It has been reported that the flow behaviour of most vegetable and fruit products deviates from the simple Newtonian behaviour (Steffe 1996). Also here, all the reconstituted suspensions and the original carrot purées listed in Table 1 turned out to be non-Newtonian liquids exhibiting a yield stress. This non-Newtonian character of the suspensions is a result of the structural modifications produced while shearing (Steffe 1996; Gallegos et al. 2004). Before giving a quantitative description of this non-Newtonian behaviour, it is visualised in Fig. 4 for several representative suspensions. From Fig. 4a, it is clear that RS_40µm(100) showed shear thinning behaviour. Also for RS_125µm(100), RS_125µm(20) and RS_250µm(20), the viscosity decreased when the shear rate ($\dot{\gamma}$) was increased from 0.1 to 100 s^{-1}. Changing particle concentration from 30 to 60 wt.% for RS_40µm(100) caused an increase in
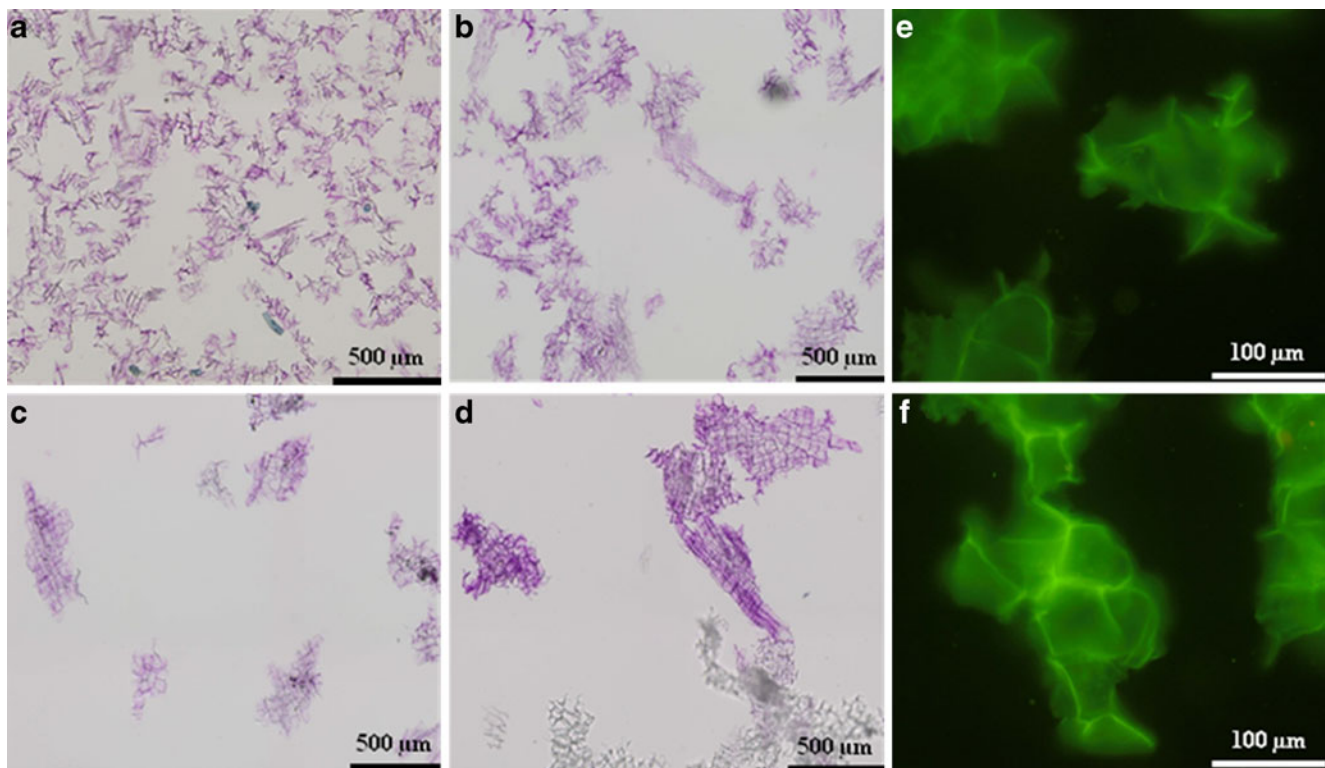
Fig. 3 Microscopic images (×10) of 1/10 diluted fractions with different particle sizes stained with toluidine blue (RS_40μm(100) (**a**), RS_125μm(100) (**b**), RS_125μm(20) (**c**) and RS_250μm(20) (**d**)) and microscopic images (×40) of 1/10 diluted RS_125μm(100) stained with acridine orange (**e** and **f**). Irregular shapes and rough edges due to cell breakage are clearly visible

viscosity with a factor of more than 100. In Fig. 4b, the appearance of a yield stress is demonstrated for all reconstituted suspensions. Particle size appears to have an effect on the magnitude of the yield stress.

*Quantitative Description of the Non-Newtonian Flow Behaviour by the Use of Predictive Models*

The flow curves were fitted to different models to investigate the influence of the particle properties (concentration and size) on the model parameters (and thus on the flow behaviour of the suspensions). Both the Bingham model (Eq. 6) and the Herschel–Bulkley model (Eq. 7) were used because these models take into account the appearance of a yield stress. However, whereas the Bingham model assumes linear flow behaviour, the Herschel–Bulkley model includes parameters to describe shear thinning or thickening. As an example, fits of both models are shown for the flow curve of suspension RS_40μm(100)_30% in Fig. 5. The Herschel–Bulkley model clearly better described the experimental flow curve (e.g. R_{adj}^2), indicating that the suspensions are no simple

Fig. 4 Non-Newtonian behaviour for several suspensions: **a** shear thinning behaviour and **b** appearance of a yield stress for the reconstituted suspensions RS_40μm(100)_30% (*filled black diamonds*), RS_40μm (100)_60% (*empty black diamonds*), RS_125μm(100) _60% (*empty black squares*), RS_125μm(20)_60% (*empty grey triangles*) and RS_250μm (20)_60% (*empty grey circles*)
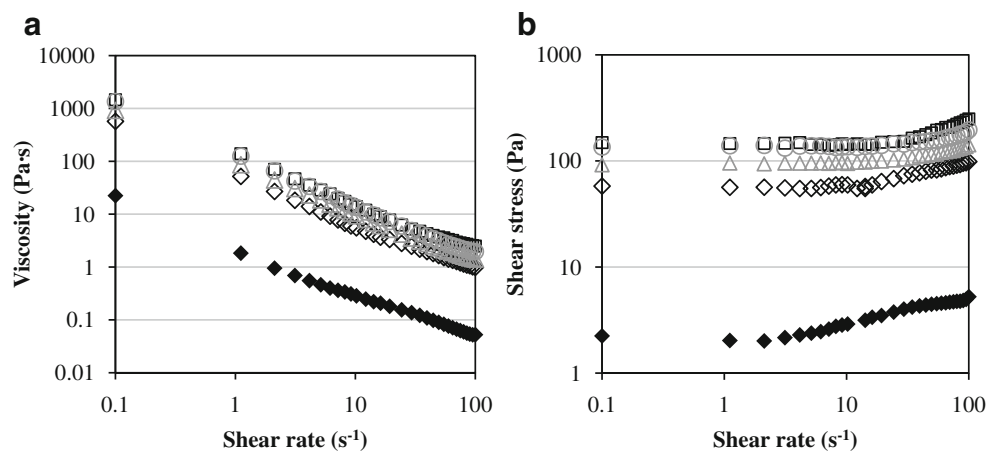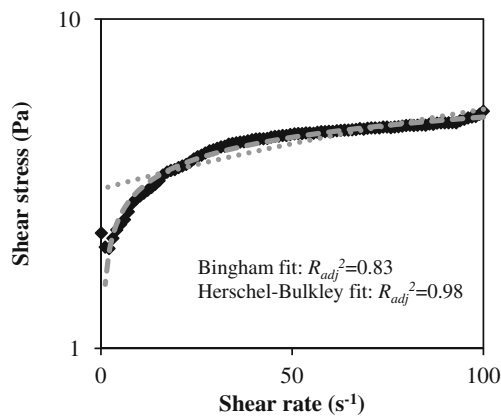
Fig. 5 Flow curve of the reconstituted suspension RS_40μm(100)_30% (*filled diamonds*) fitted with the Bingham (*dotted lines*) and Herschel–Bulkley (*dashed lines*) models

Bingham liquids. Indeed, the Herschel–Bulkley model is more often used to describe the non-Newtonian flow behaviour of dispersed food systems exhibiting a yield stress like many fruit or vegetable products (purées, juices and sauces) (Duran and Costell 1982; Steffe 1996).

The flow index (n) and the consistency coefficient (K) in the Herschel–Bulkley model were estimated by non-linear regression analysis of the experimental flow curves based on Eq. 7. Good fits of the experimental data points were obtained for all cases ($R_{adj}^2 > 0.95$). For the reconstituted suspensions, n increased with particle size and concentration, whereas no unambiguous effect of particle concentration and size on the parameter K was noticeable. When comparing n of P_100 with n of P_20, the former was smaller than the latter. Purée homogenised at a higher pressure contains less cell clusters and more small particles by result of which n decreases.

Contrary to the present results on reconstituted carrot-derived suspensions, most other studies observed a decrease of n with increasing particle concentration in plant-based suspensions (Bhamidipati and Singh 1990; Cantu-Lozano et al. 2000). However, these studies were performed on tomato sauce and apple suspensions, not on carrot-derived suspensions. Moreover, lower particle concentrations were used. Similar to the results obtained here, Sato and Cunha (2009) observed the highest n for suspensions reconstituted from jaboticaba pulp with the largest particle size. Also, Cantu-Lozano et al. (2000) concluded that n for apple dispersions with larger particles was higher. Ahmed et al. (2000), on the other hand, reported a decrease of n in chilli purée retained after using a mesh screen with large pores to prepare purée with larger particle size. In several studies on tomato suspensions, K was reported to increase with particle concentration (Rao et al. 1981; Alviar and Reid 1990; Bhamidipati and Singh 1990; Yoo and Rao 1994;

Bayod et al. 2005). Ahmed et al. (2000) observed an increase of K with increasing particle size.

As can be seen from Fig. 4a, the flow curves of the carrot-derived suspensions under investigation are highly dominated by the yield stress (straight lines with slope approximately −1). Hence, although fitting of the Herschel–Bulkley model to the flow curves was good within the range of measured shear rates, the flow behaviour at higher $\dot{\gamma}$ (> 100 s^{-1}), i.e. shear thinning, shear thickening or reaching a plateau viscosity, cannot be unambiguously predicted. Higher shear rates should be measured to estimate K and n over a wider range of shear rates, but particle inertia in the carrot-derived suspensions at shear rates above 100 s^{-1} rendered measurements at these shear rates impossible.

As mentioned above, the contribution of the yield stress to the measured viscosity is large. Therefore, in the paragraph below, the appearance of a yield stress is discussed.

The Dynamic Yield Stress

The presence of a yield stress is another rheological characteristic of concentrated suspensions and can be used as a measure for the strength of the network structure. The magnitude of the yield stress depends on the particle–particle interactions and the obtained microstructure, which are both affected by a number of factors such as particle concentration, shape, size and polydispersity (Dzuy and Boger 1983; Cheng 1986; Yoo and Rao 1994; Larson 1995; Coussot and Ancey 1999).

Because of the complexity of food systems, models such as the Bingham and Herschel–Bulkley often fail to describe the flow properties of these systems over a wide range of shear rates (Fischer et al. 2009). From Fig. 5, it was clear that the Herschel–Bulkley model was not suited to fit data points at the lowest $\dot{\gamma}$. Therefore, the dynamic yield stress (σ_{0D}) was determined for each suspension from the data points at low $\dot{\gamma}$ (as the average of the shear stress measured at shear rates 0.1, 1.11 and 2.12 s^{-1}) and not from the fitted model. Results of σ_{0D} are shown in Fig. 6a for all suspensions. σ_{0D} increased with particle concentration following a power law model:

$$\sigma_{0D} = a \cdot (\text{pulp\%})^b \tag{8}$$

The results of these fits are shown in Fig. 6a and parameter estimates for a and b are summarised in Table 3. This observed increase of yield stress with increasing particle concentration in plant-based suspensions is in agreement with a number of other studies (Yoo and Rao 1994; Yoo and Rao 1995; Bayod et al. 2007; Day et al.

Fig. 6 Average dynamic (σ_{0D}) (a) and static (σ_{0S}) (b) yield stress as a function of pulp% for the reconstituted suspensions RS_40μm(100) (*black diamonds*), RS_125μm(100) (*black squares*), RS_125μm(20) (*grey triangles*) and RS_250μm (20) (*grey circles*). *Lines* represent the power law model fits ($\sigma_0 = a \cdot (pulp\%)^b$)
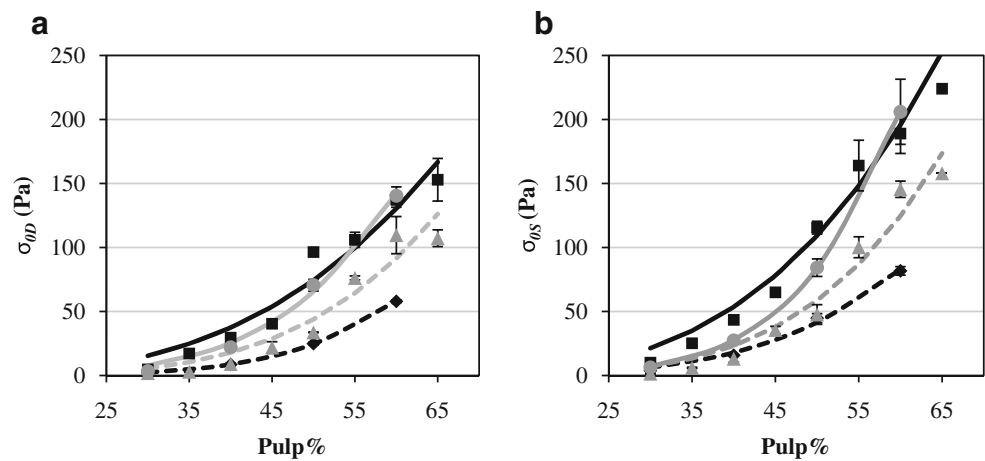
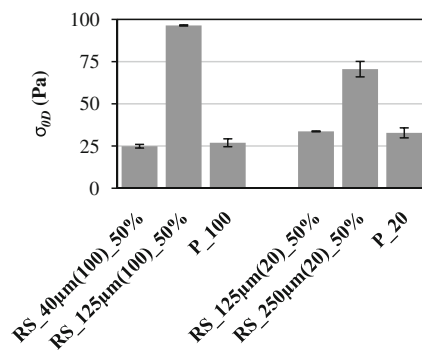2010a). Yoo and Rao (1994) also used the power law model to describe the increase of the yield stress with increasing pulp%. Since the power law exponent b is an indication of the type of network structure in the suspensions (Buscall et al. 1987; Bayod et al. 2007), the difference in exponent b for suspensions prepared from particles with different sizes can indicate differences in network structure. In Table 3, it can be observed that the power exponent b was slightly increasing when cell clusters became larger, as also observed by Day et al. (2010a). Assuming a structure of fractal aggregates, the power law exponent b can be interpreted in terms of the fractal dimension of the aggregates. Higher values of b correspond to a lower fractal dimension and hence a more open network structure (Piau et al. 1999; Mobuchon et al. 2009). However, for the relatively high volume fractions studied in the present work, contact between aggregates can occur with only a few particles per aggregate, which makes the interpretations based on fractal concepts less straightforward (Bayod and Tornberg 2011; Mewis and Wagner 2011).

The effect of particle size on σ_{0D} at constant pulp% is less clear from the present experiments. At constant pulp%, σ_{0D} for fractions made at the same homogenisation pressure decreased with decreasing particle size. In Fig. 7, this trend is shown for suspensions with a pulp% of 50 wt.%. Also, Schijvens et al. (1998) reported lower values of the yield stress in reconstituted apple sauces of smaller particle size ($d < 0.355$ mm). In most other studies, the inverse trend was reported, namely, an increase of σ_{0D} for decreasing particle size, mostly explained by the fact that smaller particles have a larger interaction surface at the same volume fraction or pulp content compared to larger particles. However, none of these studies worked with reconstituted carrot-derived suspensions and, in most cases, the yield stresses of only two particle sizes were compared, making general statements about the effect of particle size on the yield stress doubtful (Buscall et al. 1987; Qiu and Rao 1988; Yoo and Rao 1994; Cantu-Lozano et al. 2000). Moreover, in food suspensions, as the particle size changes, other particle properties such as the width of the PSD or particle shape are often changing at the same time (Tanglertpaibul and Rao 1987b). Hence, predicting the effect of individual particle properties on rheology is usually impossible. Nevertheless, some suggestions are made to explain the

Table 3 Parameters a and b (±standard error) of the power law model ($\sigma_0 = a \cdot (pulp\%)^b$) fitted to the dynamic and static yield stress as a function of the pulp%

	a	b	R_{adj}^2
Dynamic yield stress			
RS_40μm(100)	2.75E−07±1.03E−07[a]	4.68±0.09	0.99
RS_125μm(100)	4.00E−04±5.00E−04	3.08±0.28	0.94
RS_125μm(20)	6.25E−06±13.62E−06	4.03±0.53	0.90
RS_250μm(20)	4.33E−06±4.52E−06	4.23±0.26	0.99
Static yield stress			
RS_40μm(100)	1.56E−05±1.46E−05	3.78±0.23	0.99
RS_125μm(100)	4.00E−04±5.00E−04	3.20±0.22	0.98
RS_125μm(20)	5.34E−06±8.20E−06	4.14±0.37	0.95
RS_250μm(20)	3.43E−07±5.85E−07	4.94±0.42	0.98

[a] Standard error

Fig. 7 Dynamic yield stress (σ_{0D}; ±standard deviation) of the reconstituted carrot-derived suspensions and of the original carrot purées homogenised at 20 or 100 MPa, all with a pulp% of 50 wt.%

increase in σ_{0D} with increasing particle size. As aggregates, larger particles can occupy more space in the sample than aggregates of small particles due to less efficient particle packing of larger particles, leading to a larger volume effectively taken in by the aggregates of larger particles. The latter can, in turn, lead to an increase in flow resistance (Luckham and Ukeje 1999; Lopez-Sanchez et al. 2011a). Also, changes in shape and deformability of cell fragments versus cells or cell clusters may cause larger particles to occupy a larger volume whereby the yield stress increases with increasing particle size (Day et al. 2010a). Moreover, cell clusters turned out to have rough surfaces (Fig. 3) and may consequently entangle more easily, as a result of which the yield stress of cell clusters may be higher than the yield stress of cell fragments.

On the other hand, although the particle size is larger for RS_125μm(20) in comparison to that of RS_125μm(100), σ_{0D} is nevertheless smaller for RS_125μm(20) than for RS_125μm(100) at a constant pulp%. Here, the yield stress is thus decreasing with increasing particle size, which may be attributed to the larger interaction surface for smaller particles (at the same volume fraction). Besides particle size, also particle shape and type are possibly playing a role in influencing σ_{0D} and trends can thus not be explained by only one determining factor. Since variation in particle size is obtained in this case by varying the homogenisation pressure rather than the sieve size, the trend of particle shape with increasing particle size might be completely different as in the previous case. Higher homogenisation pressure appears to result in smaller but also less spherical, more irregular particles (concluded from studying several micrographs) whereby the yield stress can increase.

The σ_{0D} for P_20 and P_100 was 32.8±3.0 and 26.9± 2.3 Pa, respectively. Comparing σ_{0D} of P_20 to σ_{0D} of RS_250μm(20)_50% and σ_{0D} of P_100 to σ_{0D} of RS_125μm(100), σ_{0D} of the original carrot purées appeared to be lower than σ_{0D} of the reconstituted suspensions. Whereas $D[v,0.5]$ was almost equal for both products, the broader PSD in the original carrot purées (expressed as spread in Table 2) in comparison with the reconstituted suspensions may explain why σ_{0D} is smaller for the purées (Luckham and Ukeje 1999). Also, Sato and Cunha (2009) observed a decrease in yield stress for jaboticaba suspensions with broader PSD. In this case, smaller particles can occupy the spaces between the larger ones (Farris 1968), thereby resulting in a more efficient particle packing, whereby the volume occupied by the particles, and thus the yield stress, may decrease. Moreover, the smaller particles can serve as a lubricant between the larger ones. When comparing σ_{0D} of both original carrot purées, σ_{0D} for P_20 was higher than σ_{0D} for P_100. Possible explanations for this increase in σ_{0D} for purée made at lower pressure are the appearance of more cell clusters (thus more rough

surface) and larger average particle size (thus larger volume occupied by aggregates) in purée homogenised at lower pressure.

The Static Yield Stress

Another rheological parameter that can provide a measure of structure of the material is the static yield stress (σ_{0S}). This static yield stress (σ_{0S}) was obtained as the minimum shear stress required to induce flow in the suspension (Mewis and Macosko 1994; Steffe 1996; Barnes 1999; Moller et al. 2006). The results are shown in Fig. 6b. Similar to σ_{0D}, also σ_{0S} increased with particle concentration and, in analogy with σ_{0D}, this increase could be fitted to a power law model:

$$\sigma_{0S} = a \cdot (\text{pulp}\%)^b \tag{9}$$

The results of these fits are also shown in Fig. 6b. Parameter estimates for a and b are summarised in Table 3. Trends of σ_{0S} and power law exponent b with particle size are similar to those described for σ_{0D}. For all the reconstituted suspensions and for both original carrot purées, σ_{0S} was larger than σ_{0D}. Hence, the shear stress that is required to initiate flow is larger than the shear stress required to maintain flow at low shear rates. In a structural approach, the suspension can be assumed to consist of flocs that give the suspension a yield stress at low shear rates and form a network under quiescent conditions. The difference between σ_{0S} and σ_{0D} then provides a measure for the stress necessary to break bonds between aggregates/flocs in the network (Genovese et al. 2007). In Fig. 8, σ_{0S} is plotted versus σ_{0D}. Data points for
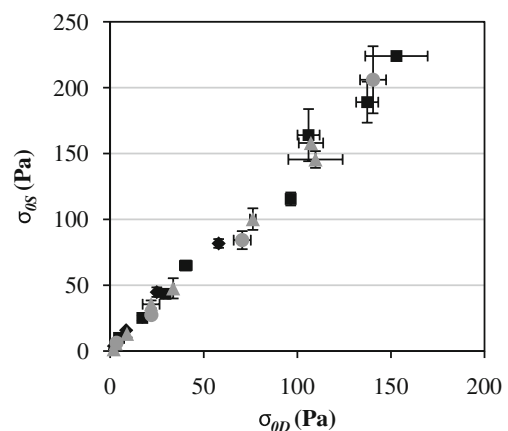
Fig. 8 Relation between the dynamic yield stress (σ_{0D}) and the static yield stress (σ_{0S}) (±standard deviation) for the reconstituted suspensions RS_40μm(100) (*black diamonds*), RS_125μm(100) (*black squares*), RS_125μm(20) (*grey triangles*) and RS_250μm(20) (*grey circles*)

all reconstituted suspensions lay on a straight line through the origin, with the ratio of σ_{0D} to σ_{0S} being approximately 0.75 for all reconstituted suspensions. This indicates that the relative contributions of the stress from the flocs (σ_{0D}) and the stress to break the bonds between the flocs in the network ($\sigma_{0S} - \sigma_{0D}$) to σ_{0S} are independent of both particle concentration and size.

Rescaling of the Viscosity Curves of the Suspensions

First, it was checked whether there is a correspondence between the steady-shear viscosity, plotted as a function of $\dot{\gamma}$, and the magnitude of the complex viscosity, plotted against the angular frequency (ω), also called the Cox–Merz rule. This empirical relationship may be useful for materials that are more easily tested under oscillatory-shear than under steady-shear conditions (Steffe 1996). If this empirical rule is valid, steady-shear measurements may be redundant and substituted by the oscillatory-shear measurements. Based on the steady-shear results from Fig. 4a and the dynamic data of Fig. 9, it could be verified that, whereas the Cox–Merz rule is often valid for simple polymeric fluids, it does not hold for the concentrated food suspensions prepared in this work. The steady-shear viscosity is thus not equal to the complex viscosity at the same $\dot{\gamma}$. This may be attributed to the fact that the microstructure present in the suspensions is altered in steady-shear tests, while dynamic testing is designed to prevent breakdown of the network structure. However, also the extended Cox–Merz rule of Doraiswamy et al. (1991), which was specially developed for highly concentrated suspensions with a yield stress, turned out not to be applicable to our suspensions.

For suspensions containing hard spherical particles, a master curve for the viscosity, independent of particle size, can be obtained by using a dimensionless shear rate or Peclet number (Pe) as the independent variable (Larson 1995). The Pe number is a dimensionless number defined as the ratio of convective to diffusive effects:

$$Pe = \frac{\eta_0 r^3 \dot{\gamma}}{kT} \tag{10}$$

with η_0 is the viscosity of suspending liquid (in pascals per second), r is the particle radius (in metres), $\dot{\gamma}$ is the shear rate (per second), k is the Boltzmann constant (1.38×10^{-23} Nm K^{-1}) and T is the absolute temperature (in kelvin).

The Pe number compares the effect of imposed shear with that of Brownian diffusion (Yoo and Rao 1994; Larson 1995). Even for the smallest particles, the Pe number was high ($>10^7$) and, therefore, it can be concluded that Brownian motion is negligible in comparison to convection. The scaling with Pe was verified for tomato purée and apple pulp suspensions (Yoo and Rao 1994; Cantu-Lozano et al. 2000) and can reduce the amount of parameters that should be studied to fully characterise food dispersions. However, scaling was not successful for the carrot-derived suspensions under investigation. At constant Pe number, the viscosity at equal values of pulp% was the highest for the reconstituted suspensions with the largest particle size. Failure of the superposition can be caused by the fact that the suspensions are not monodisperse and particle shape is more complex than for solid spheres. Also, higher particle concentrations are used in this study compared to those of Cantu-Lozano et al. (2000) or Yoo and Rao (1994). The high yield stresses of the reconstituted suspensions (Fig. 6) clearly proved that structure is present in these suspensions, which is not taken into account in the Pe number and might also cause failure of the scaling in the present work.

In conclusion, characterisation of the flow behaviour of the reconstituted carrot-derived suspensions and the original purées is clearly not straightforward. Whereas the effect of particle concentration is clear, the effect of particle size

Fig. 9 Frequency sweeps for several suspensions: **a** storage modulus (G′) and **b** loss modulus (G″) in function of the angular frequency for the reconstituted suspensions RS_40μm(100)_30% (*solid and dashed lines*), RS_40μm(100)_60% (*black and white diamonds*), RS_125μm(100)_60% (*black and white squares*), RS_125μm(20)_60% (*grey and white triangles*) and RS_250μm (20)_60% (*grey and white circles*)
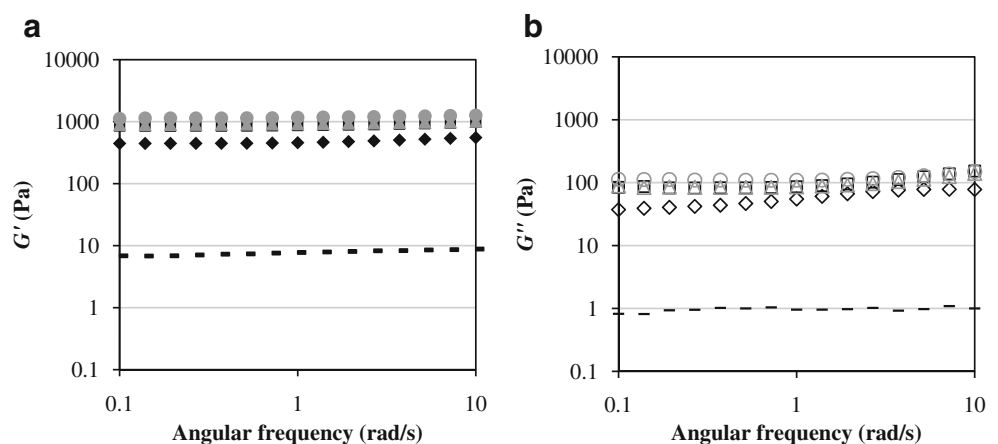
on most rheological properties (like yield stress and flow behaviour index) turned out to be difficult to be interpreted unambiguously.

Characterisation of the Viscoelastic Behaviour

To gain insight into the network structure of the plant-based suspensions, small-amplitude oscillatory tests were performed. First, results from the strain sweep were analysed to identify the linear viscoelastic region. At constant ω and low strains, the storage modulus (G') and the loss modulus (G'') were strain-independent with $G'>G''$, indicating that the suspensions behave elastically. At low strain, a zone of linear viscoelasticity was present. Increasing the strain caused a decrease in both G' and G'', whereby the zone of linear viscoelasticity ended. The limit of linearity or critical strain (γ_C) was determined experimentally as the strain beyond which G' deviated more than 5% from its linear value. Data are shown in Table 4. It can be noted that the linearity limit was low for all reconstituted suspensions and a strain of 0.1% is small enough to fall within the zone of linear viscoelasticity for all samples. For the smallest particles (RS_40μm(100)), a small decrease of γ_C was observed with increasing particle concentration. On the other hand, for larger particles, a limited increase in γ_C with increasing particle concentration was noticed. According to the fractal approach of Shih et al. (1990), this can indicate the existence of small flocs with strong links within the flocs and weak links between the flocs. Varadan and Solomon (2003) and Mason et al. (1996) explained the increase of γ_C with particle concentration by a transition from a rather heterogeneous structure at intermediate concentrations to a more homogeneous one for highly concentrated systems. In addition, for deformable particles, packing and deformation can play a role at high concentrations (Mason et al. 1996). Values of γ_C of RS_125μm(100), RS_125μm(20) and RS_250μm(20) were also small for all particle concentrations, indicating particles with a limited deformability arranged in a brittle

network. At a constant pulp%, values of γ_C of RS_40μm (100) were remarkably higher than for the suspensions with larger particles. Possibly, these small particles have more contact points than larger particles, allowing more reorganisations in the network, whereby γ_C is increasing. In addition, cell fragments may be more deformable compared to cell clusters. With regard to the original carrot purées, γ_C of P_20 was lower than γ_C of P_100, supporting the fact that γ_C increases with decreasing particle size. All in all, γ_C appeared to be less sensitive to changes in particle concentration compared to the other rheological parameters discussed so far.

Secondly, frequency sweeps at a constant strain in the linear viscoelastic region were used to characterise the network structure of the reconstituted suspensions and original carrot purées. In Fig. 9, the frequency sweeps for several representative suspensions are visualised. Suspensions had solid-like behaviour with G' larger than G'' at all ω (except for a few reconstituted suspensions with low pulp% for which G'' crossed G' at high ω). The results of the frequency sweeps were analysed using a power law model (Eqs. 11 and 12) where c, d, e and f are constants and ω is the angular frequency:

$$G' = c \cdot \omega^d \tag{11}$$

$$G'' = e \cdot \omega^f \tag{12}$$

Estimates for parameters c and e are summarised in Table 5. Values of parameters c and e increased with increasing pulp% for the reconstituted suspensions. Values of the power law exponents d and f ranged between 0.009 and 0.09 for all the reconstituted suspensions and the original carrot purées (results not shown). No unambiguous effect of particle size or concentration on exponents d and f was noticed. Because the magnitudes of G' were higher than those of G'' and the values for d and f were very small but different from zero, the rheological behaviour of these

Table 4 Strain limit of the linear viscoelastic region (γ_C; for $\omega=10$ rad/s) of all reconstituted carrot-derived suspensions and original carrot purées

Pulp% (wt.%)	γ_C (%)					
	RS_40μm(100)	RS_125μm(100)	RS_125μm(20)	RS_250μm(20)	P_20	P_100
30	1.39	0.37	0.10	0.10		
35		0.52	0.14			
40	1.00	0.52	0.27	0.37		
45		0.37	0.27			
50	0.52	0.52	0.37	0.27	0.32	0.52
55		0.52	0.37			
60	0.52	0.37	0.37	0.37		
65		0.52	0.37			

Table 5 Parameters c and e (±standard deviation) of the power law models ($G'=c\cdot\omega^d$ and $G''=e\cdot\omega^f$) fitted to the storage (G') or loss modulus (G'') as a function of the angular frequency (ω) of the reconstituted carrot-derived suspensions and original carrot purées

Pulp% (wt.%)	RS_40μm(100)	RS_125μm(100)	RS_125μm(20)	RS_250μm(20)	P_20	P_100
c						
30	7.7±0.1[a]	34.8±0.7	6.0±0.1	16.5±1.3		
35		98.6±0.2	29.7±4.9			
40	57.8±3.7	201.6±20.8	60.6±4.3	159.6±1.5		
45		272.1±7.2	211.7±0.4			
50	182.8±7.0	524.7±8.9	281.1±20.2	584.6±62.3	347.1±3.6	256.4±23.8
55		953.8±73.7	611.6±4.1			
60	479.5±6.9	978.4±139.2	909.1±46.1	1175.5±4.3		
65		1211.0±75.0	912.3±4.5			
e						
30	1.0±0.1	3.5±0.1	1.1±0.1	1.7±0.1		
35		9.4±0.1	2.9±0.4			
40	7.2±0.6	19.8±2.6	5.9±0.3	14.2±0.1		
45		27.0±0.7	20.1±1.6			
50	22.3±0.7	48.9±1.5	25.0±2.5	56.4±5.9	38.9±0.9	23.9±2.3
55		91.4±7.2	54.3±0.3			
60	56.2±1.0	93.5±13.5	87.5±10.1	117.7±1.3		
65		117.4±8.1	94.1±2.2			

[a] Standard deviation

reconstituted suspensions and original carrot purées can be described as that of weak gels. The ratio of G'/G'' at low angular frequency ($\omega=0.1$ rad/s) (Table 6) was about 10, supporting the latter conclusion (Yoo and Rao 1996; Bayod et al. 2008). Increase in particle concentration (between 30 and 65 wt.%) did not cause a transition in type of gel. However, as particle concentration increased, the weak dependency of the moduli on angular frequency was noticeable until higher ω. A negative correlation was found between G' and d, which means that, at increasing particle concentration, the suspensions evolve more towards true gels (Hill et al. 1995). Also, the network in the original carrot purées can be described as a weak gel.

Values of G' at ω of 0.1 rad/s (and parameter c) increased with increasing pulp% for the reconstituted suspensions. Consequently, the network in these suspensions is stiffer at higher particle concentration. Also, Day et al. (2010b) reported an increase of G' with particle concentration for carrot-derived suspensions. By analogy with the yield stress, this increase could be fitted to a power law model (Fig. 10):

$$G' = g \cdot (\text{pulp}\%)^h \tag{13}$$

Estimates for parameters g and h are summarised in Table 7. As exponents b (Table 3) and h (Eq. 13) showed

Table 6 G'/G'' (at $\omega=0.1$ rad/s; ±standard deviation) of reconstituted carrot-derived suspensions and original carrot purées

Pulp% (wt.%)	G'/G'' ($\omega=0.1$ rad/s)					
	RS_40μm	RS_125μm(100)	RS_125μm(20)	RS_250μm	P_20	P_100
30	8.9±0.8[a]	11.5±0.3	5.4±0.2	10.5±1.5		
35		12.0±0.3	11.1±3.0			
40	9.7±1.0	10.9±3.6	10.0±0.9	11.2±0.1		
45		9.6±0.3	10.7±0.4			
50	10.2±0.5	10.8±0.9	11.1±1.3	10.8±1.5	6.7±0.4	11.4±1.7
55		11.3±1.0	11.0±0.2			
60	11.5±0.8	10.6±1.8	10.6±1.3	9.7±0.3		
65		10.7±0.8	9.6±0.2			

[a] Standard deviation
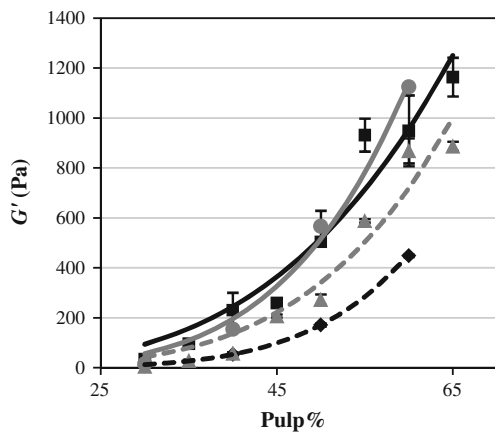
Fig. 10 Storage modulus (G') (at $\omega=0.1$ rad/s) of reconstituted carrot-derived suspensions as a function of pulp% for the reconstituted suspensions RS_40μm(100) (*black diamonds*), RS_125μm(100) (*black squares*), RS_125μm(20) (*grey triangles*) and RS_250μm (20) (*grey circles*). *Lines* represent the power law model fits ($G'=g\cdot(\text{pulp}\%)^h$)

Fig. 11 Storage modulus (G'; ±standard deviation; at $\omega=0.1$ rad/s) of the reconstituted carrot-derived suspensions and of the original carrot purées homogenised at 20 or 100 MPa, all with a pulp% of 50 wt.%

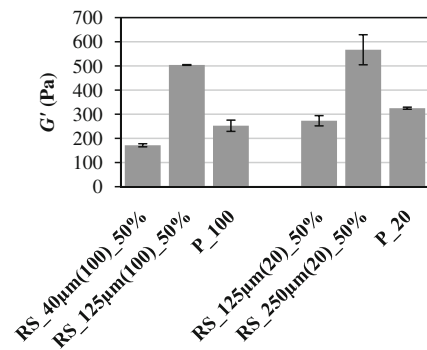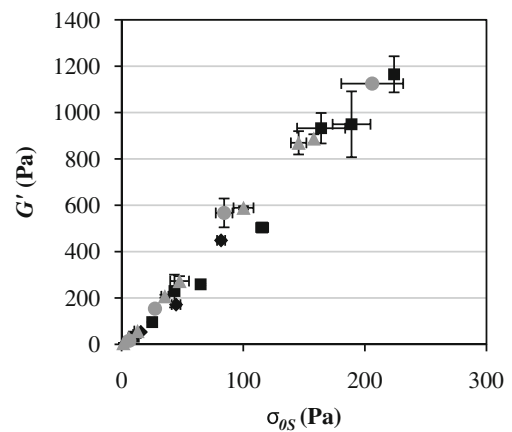comparable trends with changing particle size (except b for the power law model of σ_{0S} for RS_40μm(100)), the same trends in network structure changes between suspensions prepared from particles with different particle sizes can be seen in steady-shear and oscillatory tests (Buscall et al. 1987; Bayod et al. 2007).

Similar to the yield stress, for the reconstituted suspensions prepared from original carrot purée homogenised at the same pressure, an increase in particle size caused an increase in the value of G'. In Fig. 11, this trend is shown for suspensions with a pulp% of 50 wt.%. Similar to the conclusions for the yield stress, the effect of particle concentration on G' is clear, but the effect of particle size is more difficult to interpret. Besides particle size, also particle shape, deformability and particle surface can have a combined influence on G' and the network structure. From Fig. 11, it can also be observed that the magnitude of G' of P_20 is higher than the magnitude of P_100. This decrease in value of G' after homogenisation was also demonstrated by Lopez-Sanchez et al. (2011a) and can be explained by the decrease in particle size. In tomato purée, Bayod et al.

(2008) reported the highest value of G' for paste with the highest amount of large particles and thus the highest effective volume fraction. Values for G' of the original carrot purées homogenised at a given pressure fell between the ones of the reconstituted suspensions with a pulp% of 50 wt.% prepared from the purée homogenised at this pressure. Comparing G' of the P_20 to G' of RS_250μm (20)_50% and that of P_100 to G' of S_125(100), indeed, G' of the purée was lower than G' of the reconstituted suspension, while $D[v,0.5]$ was almost equal in both products. The larger width of the PSD in carrot purée can once again be mentioned as a possible explanation.

Because comparable trends for G' and σ_{0S} with particle concentration and size were found, the relation between G' and σ_{0S} is studied in more detail. Thereto, G' is shown as a function of σ_{0S} in Fig. 12. The ratio of σ_{0S} to G' turned out to be independent of particle size and concentration. Therefore, σ_{0S} of carrot-derived suspensions can also be obtained from oscillatory tests instead of using a stress

Table 7 Parameters g and h (±standard error) of the power law model ($G'=g\cdot(\text{pulp}\%)^h$) fitted to G' (at $\omega=0.1$ rad/s) as a function of the pulp%

	g	h	R_{adj}^2
RS_40μm(100)	1.72E−07±0.06E−07[a]	5.30±0.09	0.99
RS_125μm(100)	1.00E−03±1.90E−03	3.36±0.48	0.94
RS_125μm(20)	3.64E−05±9.85E−05	4.10±0.66	0.93
RS_250μm(20)	2.11E−05±4.03E−05	4.35±0.47	0.99

[a] Standard error

Fig. 12 Relation between the storage modulus (G') and the static yield stress (σ_{0S}; ±standard deviation) for the reconstituted suspensions RS_40μm(100) (*black diamonds*), RS_125μm(100) (*black squares*), RS_125μm(20) (*grey triangles*) and RS_250μm(20) (*grey circles*)

ramp. A similar relation was found by other authors (Larson 1995), but in the present study, the ratio σ_{0S}/G' was larger (0.16 instead of 0.01).

Conclusion

Knowing the effect of structural characteristics, such as particle properties, on the rheological behaviour of food suspensions may enable the design of production processes for materials with tailored properties. From this study, particle properties are shown to have a major impact on the rheological properties of particulated, plant-based food systems, such as carrot-derived suspensions. However, the rheology of these suspensions appeared to be complex because suspensions are non-Newtonian liquids exhibiting a yield stress. Besides this complex rheological behaviour, often a combination of particle properties (like particle type, size and size distribution) appeared to influence the rheology whereby it was not always possible to assign changes in rheological properties to a single particle property. If particles would be spherical with smooth surfaces, rheological properties would be determined exclusively by particle size and PSD (Lopez-Sanchez 2011). Here, microscopic images showed that the particles are no perfect spheres and have ragged, irregular surfaces. Therefore, interactions between particles are more complex and rheological parameters are also influenced by the particle shape and the particle surface, rendering the prediction of rheological parameters on the basis of the particle properties even more complex. In most cases (like for the yield stress, storage modulus, flow index) unambiguous relations between particle concentration and rheological properties of suspensions could be found. However, relations between the particle size and most rheological parameters are less clear because the particle shape, surface and size distribution are also influencing the rheological properties at the same time.

Flow curves were dominated by yield stress. Network stiffness, measured as the yield stress or the storage modulus, increased with increasing particle concentration for all the carrot-derived suspensions and this increase could be fitted to a power law model. Exponents of these models demonstrate that network structure is changing in suspensions when particle size is altered. The ratios of σ_{0D} to σ_{0S} and σ_{0S} to G' turned out to be independent of particle size and concentration. Changing particle size or concentration did not significantly change the gel type. All systems could be described as weak gels. Nevertheless, gelling behaviour was noticeable until higher angular frequencies at higher particle concentrations.

In future investigations, it can be useful to look more in detail into the effect of particle type and shape on the

rheology of carrot-derived suspensions. Nevertheless, by changing the particle type, the particle size is also often changed and it will be a challenge to study the effect of both structural properties separately on the rheological parameters.

References

Ahmed, J., Shivhare, U. S., & Raghavan, G. S. V. (2000). Rheological characteristics and kinetics of colour degradation of green chilli puree. *Journal of Food Engineering, 44*(4), 239–244.

Alviar, M. S. B., & Reid, D. S. (1990). Determination of rheological behavior of tomato concentrates using back extrusion. *Journal of Food Science, 55*(2), 554–555.

Anthon, G. E., Diaz, J. V., & Barrett, D. M. (2008). Changes in pectins and product consistency during the concentration of tomato juice to paste. *Journal of Agricultural and Food Chemistry, 56*(16), 7100–7105.

Barnes, H. A. (1999). The yield stress—A review or 'pi alpha nu tau alpha rho epsilon iota'—Everything flows? *Journal of Non-Newtonian Fluid Mechanics, 81*(1–2), 133–178.

Bayod, E., Bolmstedt, U., Innings, F., & Tornberg, E. (2005). Rheological characterization of fiber suspensions prepared from vegetable pulp and dried fiber: A comparative study. *Annual Transactions of the Nordic Rheology Society, 13*, 249–253.

Bayod, E., Mansson, P., Innings, F., Bergenstahl, B., & Tornberg, E. (2007). Low shear rheology of concentrated tomato products. Effect of particle size and time. *Food Biophysics, 2*(4), 146–157.

Bayod, E., & Tornberg, E. (2011). Microstructure of highly concentrated tomato suspensions on homogenisation and subsequent shearing. *Food Research International, 44*(3), 755–764.

Bayod, E., Willers, E. P., & Tornberg, E. (2008). Rheological and structural characterization of tomato paste and its influence on the quality of ketchup. *LWT- Food Science and Technology, 41*(7), 1289–1300.

Beresovsky, N., Kopelman, I. J., & Mizrahi, S. (1995). The role of pulp interparticle interaction in determining tomato juice viscosity. *Journal of Food Processing and Preservation, 19*(2), 133–146.

Bhamidipati, S., & Singh, R. K. (1990). Flow behavior of tomato sauce with or without particulates in tube flow. *Journal of Food Process Engineering, 12*(4), 275–293.

Buscall, R., McGowan, I. J., Mills, P. D. A., Stewart, R. F., Sutton, D., White, L. R., et al. (1987). The rheology of strongly-flocculated suspensions. *Journal of Non-Newtonian Fluid Mechanics, 24*(2), 183–202.

Cantu-Lozano, D., Rao, M. A., & Gasparetto, C. A. (2000). Rheological properties of noncohesive apple dispersion with helical and vane impellers: Effect of concentration and particle size. *Journal of Food Process Engineering, 23*(5), 373–385.

Cheng, D. C. H. (1986). Yield stress—A time-dependent property and how to measure it. *Rheologica Acta, 25*(5), 542–554.

Coussot, P., & Ancey, A. (1999). Rheophysical classification of concentrated suspensions and granular pastes. *Physical Review E, 59*(4), 4445–4457.

Day, L., Xu, M., Oiseth, S. K., Hemar, Y., & Lundin, L. (2010). Control of morphological and rheological properties of carrot cell wall particle dispersions through processing. *Food and Bioprocess Technology, 3*(6), 928–934.

Day, L., Xu, M., Oiseth, S. K., Lundin, L., & Hemar, Y. (2010). Dynamic rheological properties of plant cell-wall particle dispersions. *Colloids and Surfaces. B, Biointerfaces, 81*(2), 461–467.

Den Ouden, F. W. C., & Van Vliet, T. (1997). Particle size distribution in tomato concentrate and effects on rheological properties. *Journal of Food Science, 62*(3), 565–567.

Den Ouden, F. W. C., & Van Vliet, T. (2002). Effect of concentration on the rheology and serum separation of tomato suspensions. *Journal of Texture Studies, 33*(2), 91–104.

Doraiswamy, D., Mujumdar, A. N., Tsao, I., Beris, A. N., Danforth, S. C., & Metzner, A. B. (1991). The Cox–Merz rule extended—A rheological model for concentrated suspensions and other materials with a yield stress. *Journal of Rheology, 35*(4), 647–685.

Duran, L., & Costell, E. (1982). Rheology of apricot puree—Characterization of flow. *Journal of Texture Studies, 13*(1), 43–58.

Dzuy, N. Q., & Boger, D. V. (1983). Yield stress measurement for concentrated suspensions. *Journal of Rheology, 27*(4), 321–349.

Errington, N., Tucker, G. A., & Mitchell, J. R. (1998). Effect of genetic down-regulation of polygalacturonase and pectin esterase activity on rheology and composition of tomato juice. *Journal of the Science of Food and Agriculture, 76*(4), 515–519.

Farris, R. J. (1968). Prediction of the viscosity of multimodal suspensions from unimodal viscosity data. *Transactions of the Society of Rheology, 12*(2), 281–301.

Fischer, P., Pollard, M., Erni, P., Marti, I., & Padar, S. (2009). Rheological approaches to food systems. *Comptes Rendus Physique, 10*(8), 740–750.

Gallegos, C., Franco, J.M. & Partal, P. (2004). Rheology of food dispersions. *Rheology Reviews* 19–65.

Genovese, D. B., Lozano, J. E., & Rao, M. A. (2007). The rheology of colloidal and noncolloidal food dispersions. *Journal of Food Science, 72*(2), R11–R20.

Hill, M. A., Mitchell, J. R., & Sherman, P. A. (1995). The relationship between the rheological and sensory properties of a lemon pie filling. *Journal of Texture Studies, 26*(4), 457–470.

Horwitz, W. (1980). *Official methods of analysis of the Association of Official Analytical Chemists* (pp. 1–970). Washington: Association of Official Analytical Chemists.

Larson, R. G. (1995). *Structure and Rheology of Complex Fluids* (pp. 1–663). New York: Oxford University Press.

Lopez-Sanchez, P. (2011). Microstructure and rheological properties of plant particle suspensions prepared using different physical treatments. Ph.D. Thesis, Department of Chemical and Biological Engineering, Chalmers University of Technology, Göteborg, Sweden.

Lopez-Sanchez, P., Nijsse, J., Blonk, H. C. G., Bialek, L., Schumm, S., & Langton, M. (2011). Effect of mechanical and thermal treatments on the microstructure and rheological properties of carrot, broccoli and tomato dispersions. *Journal of the Science of Food and Agriculture, 91*(2), 207–217.

Lopez-Sanchez, P., Svelander, C., Bialek, L., Schumm, S., & Langton, M. (2011). Rheology and microstructure of carrot and tomato emulsions as a result of high-pressure homogenization conditions. *Journal of Food Science, 76*(1), E130–E140.

Luckham, P. F., & Ukeje, M. A. (1999). Effect of particle size distribution on the rheology of dispersed systems. *Journal of Colloid and Interface Science, 220*(2), 347–356.

Mason, T. G., Bibette, J., & Weitz, D. A. (1996). Yielding and flow of monodisperse emulsions. *Journal of Colloid and Interface Science, 179*(2), 439–448.

Mewis, J., & Macosko, C. W. (1994). Suspension rheology. In C. W. Macosko (Ed.), *Rheology principles, measurements and applications* (pp. 425–474). New York: VCH.

Mewis, J., & Wagner, N. J. (2011). *Colloidal suspension rheology* (pp. 1–393). New York: Cambridge University Press.

Mobuchon, C., Carreau, P. J., & Heuzey, M. C. (2009). Structural analysis of non-aqueous layered silicate suspensions subjected to shear flow. *Journal of Rheology, 53*(5), 1025–1048.

Moller, P. C. F., Mewis, J., & Bonn, D. (2006). Yield stress and thixotropy: On the difficulty of measuring yield stresses in practice. *Soft Matter, 2*(4), 274–283.

Ovarlez, G., Mahaut, F., Bertrand, F., & Chateau, X. (2011). Flows and heterogeneities with a vane tool: Magnetic resonance imaging measurements. *Journal of Rheology, 55*(2), 197–223.

Piau, J. M., Dorget, M., & Palierne, J. F. (1999). Shear elasticity and yield stress of silica-silicone physical gels: Fractal approach. *Journal of Rheology, 43*(2), 305–314.

Qiu, C. G., & Rao, M. A. (1988). Role of pulp content and particle-size in yield stress of apple sauce. *Journal of Food Science, 53*(4), 1165–1170.

Rao, M. A. (1987). Predicting the flow properties of food suspensions of plant-origin. *Food Technology, 41*(3), 85–88.

Rao, M. A. (2007). *Rheology of fluid and semisolid foods: Principles and applications* (pp. 1–462). Washington: Springer.

Rao, M. A., Bourne, M. C., & Cooley, H. J. (1981). Flow properties of tomato concentrates. *Journal of Texture Studies, 12*(4), 521–538.

Sato, A. C., & Cunha, R. L. (2009). Effect of particle size on rheological properties of jaboticaba pulp. *Journal of Food Engineering, 91*(4), 566–570.

Schijvens, E. P. H. M., Van Vliet, T., & van Dijk, C. (1998). Effect of processing conditions on the composition and rheological properties of applesauce. *Journal of Texture Studies, 29*(2), 123–143.

Servais, C., Jones, R., & Roberts, I. (2002). The influence of particle size distribution on the processing of food. *Journal of Food Engineering, 51*(3), 201–208.

Shih, W. H., Shih, W. Y., Kim, S. I., Liu, J., & Aksay, I. A. (1990). Scaling behavior of the elastic properties of colloidal gels. *Physical Review A, 42*(8), 4772–4779.

Steffe, J. F. (1996). *Rheological Methods in Food Processing Engineering* (pp. 1–418). Michigan: Freemann Press.

Tabilo-Munizaga, G., & Barbosa-Canovas, G. V. (2005). Rheology for the food industry. *Journal of Food Engineering, 67*(1–2), 147–156.

Tanglertpaibul, T., & Rao, M. A. (1987a). Flow properties of tomato concentrates—Effect of serum viscosity and pulp content. *Journal of Food Science, 52*(2), 318–321.

Tanglertpaibul, T., & Rao, M. A. (1987b). Rheological properties of tomato concentrates as affected by particle-size and methods of concentration. *Journal of Food Science, 52*(1), 141–145.

Valencia, C., Sanchez, M. C., Ciruelos, A., Latorre, A., Madiedo, J. M., & Gallegos, C. (2003). Non-linear viscoelasticity modeling of tomato paste products. *Food Research International, 36*(9–10), 911–919.

Varadan, P., & Solomon, M. J. (2003). Direct visualization of long-range heterogeneous structure in dense colloidal gels. *Langmuir, 19*(3), 509–512.

Yoo, B., & Rao, M. A. (1994). Effect of unimodal particle-size and pulp content on rheological properties of tomato puree. *Journal of Texture Studies, 25*(4), 421–436.

Yoo, B., & Rao, M. A. (1995). Yield stress and relative viscosity of tomato concentrates—Effect of total solids and finisher screen size. *Journal of Food Science, 60*(4), 777–779.

Yoo, B., & Rao, M. A. (1996). Creep and dynamic rheological behavior of tomato concentrates: Effect of concentration and finisher screen size. *Journal of Texture Studies, 27*(4), 451–459.

Zdunek, A., Konskyy, R., Cybulska, J., Konstankiewicz, K., & Umeda, M. (2007). Visual texture analysis for cell size measurements from confocal images. *International Agrophysics, 21*(4), 409–414.